

Mapping the frontiers of the nuclear mass surface

Zach Meisel

Institute of Nuclear & Particle Physics, Department of Physics & Astronomy, Ohio University, Athens, OH, 45701 USA

E-mail: meisel@ohio.edu

October 2019

Abstract. Nuclear masses play a central role in nuclear astrophysics, significantly impacting the origin of the elements and observables used to constrain ultradense matter. A variety of techniques are available to meet this need, varying in their emphasis on precision and reach from stability. Here I briefly summarize the status of and near-future for the time-of-flight magnetic-rigidity (TOF- $B\rho$) mass measurement technique, emphasizing the complementary and interconnectedness with higher-precision mass measurement methods. This includes of recent examples from TOF- $B\rho$ mass measurements that map the evolution of nuclear structure across the nuclear landscape and significantly impact the results and interpretation of astrophysical model calculations. I also forecast expected expansion in the known nuclear mass surface from future measurement at the Facility for Rare Isotope Beams.

1. Introduction

Nuclear masses, and more specifically nuclear mass differences, are fundamental descriptors of atomic nuclei. Mass differences reflect the evolving energetics associated with changes in nuclear structure across the nuclear landscape as well as the energy costs (and gains) for nuclear reactions in astrophysical environments. Typical mass differences of interest are separation energies, e.g. for two-neutrons,

$$S_{2n}(Z, N) = ME(Z, N - 2) + 2ME(0, 1) - ME(Z, N) \quad (1)$$

and the reaction Q -value

$$Q = \Sigma_{\text{reactants}} ME - \Sigma_{\text{products}} ME, \quad (2)$$

where ME is the atomic mass excess, Z is the proton number, and N is the neutron number. Changes in the slope of S_{2n} for neutron-rich isotopes of an element provide signatures of neutron shell and subshell closures, while Q -values are essential inputs into astrophysics model calculations.

Therefore, nuclear mass measurements continue to play an essential role in nuclear physics studies, in particular for nuclear structure and nuclear astrophysics. Recent contributions include the emergence of the $N = 32$ [1] and $N = 34$ shell closures [2],

mapping the island of inversion near $N = 40$ [3], Q -value determinations essential for calculations of type-I X-ray bursts [4, 5], and determining the trend in masses of neutron rich nuclei whose imprint can be seen in calculations of astrophysical r -process abundance patterns [6, 7].

In all of these cases, precise nuclear mass determinations were required to contribute to solving the problem at hand. However, it is important to note that “precision” is a relative concept, where the necessary mass precision for a given scenario depends on the context. For instance, consider the case of $^{36}\text{Ar}(p, \gamma)$, whose dependence on a single low-energy resonance means that keV-level changes to the Q -value leads to tens of percent changes in the astrophysical reaction rate [8]. Near the other extreme is the much lower precision required to constrain the properties of the neutron star crust. As an example, Figure 1 show the equilibrium composition for a cold-catalyzed neutron star crust using various nuclear mass models. Here MeV-level differences between nuclear masses are required to modify the onset of the $N = 82$ shell closure, to which the composition converges deep in the outer crust.

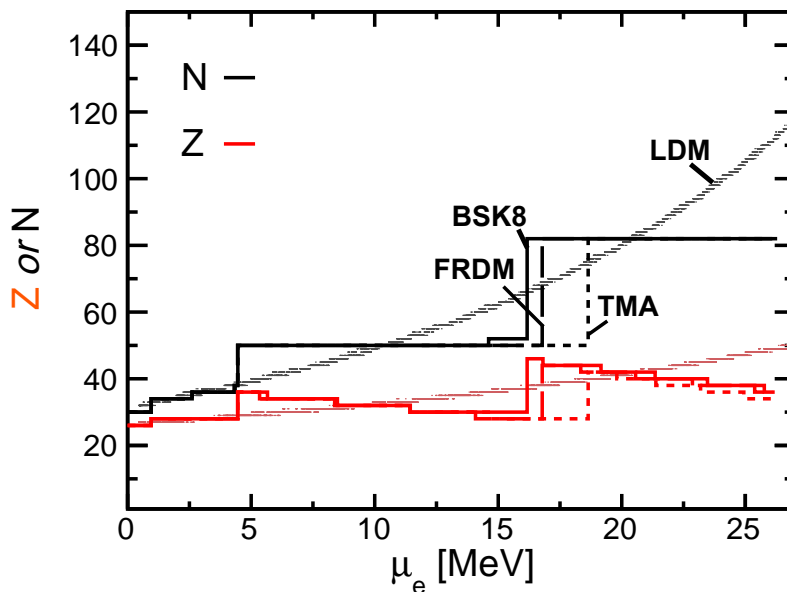


Figure 1. Equilibrium neutron number N and proton number Z for depths in a non-accreting neutron star as indicated by the electron chemical potential μ_e . Data are from References [9] and [10].

The precision that can be achieved in nuclear mass measurement varies for the available measurement techniques, where the cost of increased precision is often increased measurement time. A map of achieved measurement precision for nuclides of various half-lives is shown in Figure 3 of Reference [11]. While a nuclear mass m precision of $(\delta m)/m < 10^{-8}$ has been achieved for penning trap mass spectrometry (PTMS), this is in general only possible for a half-life $t_{1/2} > 1$ s. For the shortest $t_{1/2}$

and lowest production rates, the time-of-flight magnetic-rigidity (TOF- $B\rho$) method can be used, albeit at the cost of precision. The TOF- $B\rho$ method is generally limited to a precision of a few times 10^{-6} .

The value of a relatively low-precision mass measurement technique can be seen by considering the characteristics of nuclides of interest for astrophysical processes. The difficulty of measuring a nuclide in the laboratory can be quantified using the exoticity [12],

$$\varepsilon = \log_{10} \left| \frac{dN_{\text{stab}}}{t_{1/2}(dN_{\text{drip}} + 1)} \right|, \quad (3)$$

where dN_{stab} is the number of neutrons from stability along an isotopic chain and dN_{drip} is the same for the neutron dripline, e.g. as defined by the FRDM [13] mass model. Typically (see Figure 6 of Reference [12]), PTMS is limited to $\varepsilon < 1$, while TOF- $B\rho$ probes out to roughly $\varepsilon = 4$. For context, consider the ε distributions for nuclides involved in astrophysical processes shown in Figure 2. It is clear that measurement techniques accessing $\varepsilon > 1$ are essential to fully map the nuclear mass surface in the region of interest for astrophysical processes involving neutron-rich nuclides.

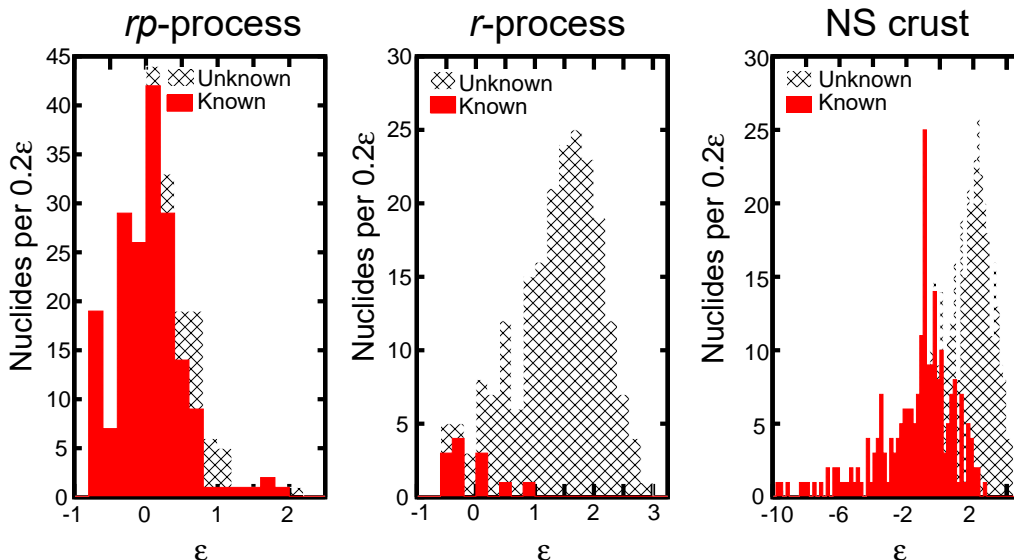


Figure 2. Nuclides involved in astrophysical processes with known (solid-red) or unknown (hatched black) nuclear mass, binned by ε . The rp , r , and neutron star crust reaction network paths are from References [14], [15], and [16], respectively.

The remainder of this article focuses on the TOF- $B\rho$ mass measurement method. Section 2 briefly summarizes the TOF- $B\rho$ method, Section 3 highlights some significant contributions of TOF- $B\rho$ measurements to nuclear structure and nuclear astrophysics, and Section 4 provides a preview of mass measurement achievements anticipated at the upcoming Facility for Rare Isotope Beams (FRIB).

2. The TOF- $B\rho$ mass measurement method

The concept for the TOF- $B\rho$ method is that the nuclear mass can be determined by equating the centripetal and Lorentz forces on a charged massive particle (i.e. a nucleus) moving through a magnetic system. After some straightforward algebra and applying a relativistic correction in the form of the Lorentz factor γ , it is apparent that the rest mass

$$m_0 = \frac{\text{TOF } qB\rho}{L_{\text{path}} \gamma}, \quad (4)$$

where TOF is the time-of-flight along a path of length L_{path} for an ion with charge q and magnetic rigidity $B\rho$. In practice, this relationship is not practicable for nuclear mass determinations of the necessary precision. For instance, for the typical conditions of a TOF- $B\rho$ experiment [17], using Equation 4 to determine a nuclear mass to the 10^{-6} -level would require knowing $L_{\text{path}} \sim 60$ m to tens of microns. Instead, an empirical relation is established by determining the $B\rho$ -corrected TOF, TOF' , of several nuclides whose mass is known, e.g. from PTMS, to high-precision:

$$m_0 = f(Z, A = Z + N, \text{TOF}'). \quad (5)$$

Ultimately, the empirical approach requires determining the average TOF within less than a picosecond and $B\rho$ via a sub-millimeter measurement of the vertical displacement at a dispersive focus for several tens of nuclides. Ideally, the nuclides whose mass is known (“reference nuclides”) have Z and A/Z similar to the nuclides of interest.

Uncertainty quantification in the TOF- $B\rho$ method provides a significant challenge, due to the careful consideration required to assign systematic uncertainties. To aid in this discussion, consider the Rumsfeld Quadrant [18] shown in Figure 3.

| | |
|-------------------------------|------------------------------------|
| Known Knowns | Unknown Knowns |
| Calibration Masses | Systematic Spread in Fit Residuals |
| Known Unknowns | Unknown Unknowns |
| Uncertainty in Fit Parameters | Uncertainty in Fit Function |

Figure 3. TOF- $B\rho$ mass measurement uncertainty considerations categorized via a Rumsfeld Quadrant, following Reference [18].

Masses of reference nuclides provide known knowns through which to calibrate Equation 5. Naturally, the fit parameters for this equation have uncertainties which can be determined via standard error propagation, or, to ensure adequate accounting of numerous multi-collinearities, via a Monte Carlo technique as in Reference [17]. These are the known unknowns.

Systematic uncertainties of two distinct types often dominate the final mass uncertainty (for nuclides with greater than ~ 500 counts). An unknown that we know of is the systematic spread remaining in the residuals of the fit to reference nuclides which nearly always have $\chi_\nu^2 > 1$. This uncertainty is generally accounted for by adding a blanket uncertainty in m/q (as the actual fit function used determines this quantity) until $\chi_\nu^2 = 1$. The second, and unfortunately often omitted, systematic uncertainty comes from the unknown unknown: we do not know if the relation ultimately used in Equation 5 is the fit-function that best describes the data. While Occam's razor dictates that the simplest model should be preferred, this simplicity needs to be balanced with the quality of the overall fit. A suggested approach is to use $\Delta\chi^2 = \chi_i^2 - \chi_{\min}^2$, where χ_i^2 applies to a given model and χ_{\min}^2 is the model resulting in the overall best-fit. The set of fit-functions which nominally describe the data equally well within some degree of confidence can be determined using $\Delta\chi^2$ tabulated for the number of degrees of freedom [19].

3. TOF- $B\rho$ contributions to nuclear structure and nuclear astrophysics

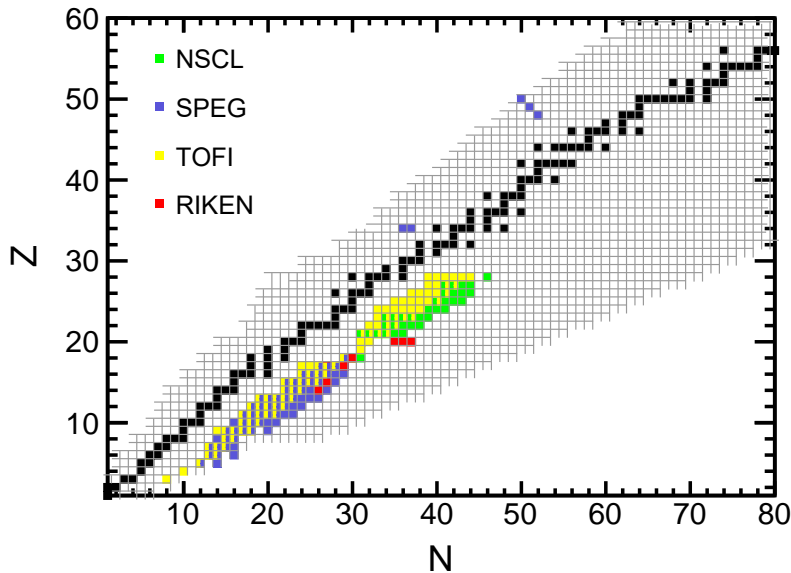


Figure 4. Nuclear masses measured by the TOF- $B\rho$ method at the NSCL [20], SPEG at GANIL [21], TOFI at LAMPF [22], and RIKEN [2].

More than 300 nuclear masses have been determined using the TOF- $B\rho$ method,

corresponding to a total of roughly 150 nuclides. Figure 4 shows these contributions by facility. Early measurements were performed using SPEG at GANIL [21] and TOFI at the LAMPF [22] facility, though neither set-up is still operational. In the past decade, TOF- $B\rho$ has been employed at NSCL [20] and RIKEN [2]. The concentration of measurements for $Z < 30$ is largely due to the difficulty of dealing with multiple charge-states present for studies of higher- Z nuclides, though efforts are ongoing to address this difficulty, e.g. using the technique of Reference [23].

Nuclear structure studies have identified regions of shape coexistence, the appearance and disappearance of shell closures, and the existence of halo nuclides. For instance, the lower-bound of the $N = 28$ shell closure was mapped by References [24, 25, 26]. The properties of halo nuclides were determined by References [22, 27], where the latter was key to establishing the two-neutron halo nature of ^{22}C and one-neutron halo of ^{31}Ne .

Achievements in nuclear astrophysics have largely focused on improving models of the accreted neutron star crust, where nuclear masses determine the location and strength of heat sources and heat sinks occurring due to electron-capture reactions [9]. Thus far, measurement results [17, 28] have indicated that electron-capture heat sources appear to be weaker than previously predicted. However, the accreted neutron star crust is not as cool as was once thought possible, since Reference [29] found that the strongest predicted heat sink in fact does not exist. Work is ongoing to expand TOF- $B\rho$ studies of astrophysical interest to the r -process region [30].

4. The future of TOF- $B\rho$ mass measurements

While a handful of measurement targets remain at existing facilities, to significantly extend the TOF- $B\rho$ method to more exotic isotopes will require state-of-the-art radioactive ion beam facilities, such as FRIB. The purpose of this section is to forecast the extent to which the known nuclear mass surface is likely to be expanded at FRIB by coordinated efforts in TOF- $B\rho$ and PTMS measurements. This is done by discussing predicted FRIB production rates followed by anticipated achievements in PTMS, TOF- $B\rho$, and the two techniques combined.

4.1. FRIB production rates

FRIB production rate predictions[‡] are calculated using the software from Reference [31], whose assumptions are briefly described here. Fast-beam rates, required for TOF- $B\rho$, were calculated employing the KTUY mass model [32], EPAX 2.15 fragmentation cross section parameterization [33], LISE++3EER model for production cross sections from in-flight fission [34], and LISE++v9.2.68 for beam transmission efficiency [35]. In each case the rate chosen is that from the optimum primary beam, i.e. the one of the 47

[‡] At present, calculations for individual nuclides can be obtained at <https://groups.nsl.msu.edu/frib/rates/fribrates.html>.

anticipated primary beams producing the highest rate, and a beam power of 400 kW. For the case of stopped beams, which are required for PTMS, the beam rate is reduced by the gas-stopping efficiency ($\sim 1-50\%$, depending on the ion mass and incident beam-rate), the radioactive decay of ions during the 0.05 s extraction time, and the transport efficiency from the gas-stopper to the downstream charge-breeder, which is assumed to be 80% [31].

Fast beam rates of roughly 10^8 particles per second (pps) are anticipated for nuclides just beyond the present limit of known masses, where the production rate generally drops off one order of magnitude for every 1-2 additional neutrons from stability. The stopped-beam rate is 10% of the fast-beam rate on average, but mostly ranges from 0-40% (0% cases are due to short half-lives).

4.2. Penning trap mass measurement

PTMS, the highest-precision mass measurement technique presently available for rare isotopes, will be performed with the Low Energy Beam Ion Trap (LEBIT) Penning trap at FRIB [36]. The PTMS technique consists of obtaining nuclear masses by measuring the resonant frequency of the nucleus of interest with respect to the resonant frequency for an ion (or typically atomic cluster) of known mass orbiting within a few cubic-centimeter volume, confined by a strong magnetic field and hyperbolic electrodes [37]. PTMS has been demonstrated to deliver a mass measurement precision of 10^{-6} or better for as little as ~ 50 measured ions [38] and for nuclides with half-lives as short as ~ 10 ms [39].

The time-of-flight ion-cyclotron-resonance (TOF-ICR) technique is predominantly employed for PTMS. For TOF-ICR PTMS, the cyclotron resonance of the ion in the trap, which is directly proportional to its mass, is identified by converting the orbital motion in the trap to a longitudinal motion out of the trap and finding the minimum TOF to a fixed detection location. The measurement uncertainty for TOF-ICR is reduced by storing individual ions for long times in the trap and observing several ions over a large enough frequency range to map the cyclotron resonance. The relative statistical uncertainty $\delta m/m$, which is generally much larger than the systematic uncertainty for PTMS of rare isotopes, is roughly given by $\delta m/m \approx R^{-1}n^{-1/2}$, where n is the number of ions detected and R is the resolving power [40]. The resolving power is approximately equal to the product of the cyclotron frequency of the ion in the trap f_c (typically $\mathcal{O} \sim \text{MHz}$) and the length of time the ion orbits in the trap t_{obs} (typically $\mathcal{O} \sim 0.1$ s). R therefore depends on many considerations, such as the mass of the nucleus of interest, the obtainable charge-state, the time it takes to produce the optimum charge state, and the nuclear half-life.

Given the uncertainties in charge-breeding capabilities and the approximate nature of the estimate for n , I make the approximation that $R = 10^5$ for all nuclides of interest, which is in-line with sample cases for rare isotopes [41]. For simplicity, I assume $t_{\text{obs}}=100$ ms, and therefore n will be the product of the stopped-beam rate

and the duration of the experiment, reduced due to the radioactive decay of ions during the measurement process. For the experiment duration, I assume 24 hours of measurement time for the ion of interest, as is typical for PTMS measurements of exotic nuclides. Experimental β -decay half-lives from Reference [42] are used when available and predictions from Reference [43] are used otherwise. I assume a systematic uncertainty typical for the measurement precision of reference ions, $\delta m/m = 10^{-8}$ [44].

Above $A \approx 50$, the known mass surface will be extended by PTMS by a few isotopes or more for each isotopic chain. The improvement over current nuclear mass uncertainties is also significant, considering that many nuclear masses at the present experimental frontier are only known to precisions of $\delta m/m \approx 10^{-5}$ [45]. The greatest gains are expected for neutron-rich isotopes with $Z > 55$, which will substantially improve the predictive power of rare-earth element nucleosynthesis in the r -process [46]. Note that the predicted gains on the proton-rich side are unreliable, as particle-decays are not taken into account in our estimates. Furthermore, the estimates neglect the potential existence of isomeric states and isobaric contaminants [47]; however, recent improvements in PTMS, such as the stored waveform inverse fourier transform [48] and phase-imaging ion-cyclotron-resonance [49] techniques will mitigate the impact of these complications. Additionally, the reach of PTMS may be extended by near-future developments such as the single ion penning trap (SIPT) method [44]; however, expectations for SIPT have yet to be benchmarked with rare isotope measurements and so are not considered here.

4.3. TOF- $B\rho$ mass measurement

The TOF- $B\rho$ method is described in Section 2. The details of the uncertainty evaluation are elaborated upon here as they are pertinent to developing a forecast of anticipated measurement results. It is important to note that the TOF- $B\rho$ method relies on the availability of PTMS results for nuclides nearby (in terms of Z and N) the isotopes of interest and is primarily used as a tool to extend the known mass surface by a few more neutrons along an isotopic chain.

Unlike PTMS, the measurement uncertainty of TOF- $B\rho$ is generally dominated by systematic uncertainties due the many unknowns which must be accounted for along the large experimental set-ups [17, 40]. Therefore, the estimation technique for the mass measurement uncertainty achievable via TOF- $B\rho$ is somewhat more approximate. The statistical uncertainty of TOF- $B\rho$ is related to the TOF measurement precision $\sigma_{\text{TOF}}/\text{TOF}$ and number of measured ions n by $\delta m/m \approx \sigma_{\text{TOF}}/(\text{TOF}\sqrt{n})$, where a typical $\sigma_{\text{TOF}}/\text{TOF}$ of 10^{-4} [50, 28, 26] is assumed here. I base the systematic uncertainty on the rough empirically motivated approximation§ [17, 26, 27, 28, 29, 50] that $\delta m/m|_{\text{sys}} = 5 \times 10^{-6}(1 + (N - N_{\text{ref}}))$, where $N - N_{\text{ref}}$ is the number of neutrons separating the nuclide of interest and the most neutron-rich isotope of that element with

§ Note that the true systematic uncertainty depends on many factors, not least the details of the local TOF-mass relationship and the availability of suitable reference nuclides [17].

a mass uncertainty $\leq 10^{-6}$. I sum the statistical and systematic uncertainties to arrive at a total uncertainty and assume a measurement time of 100 hours, as is typical for recent TOF- $B\rho$ experiments.

In general TOF- $B\rho$ extends the measurable mass surface by 1-3 nuclides with a precision useful to applications in nuclear structure and nuclear astrophysics (\lesssim a few times 10^{-5}). The given estimates ignore potential complications such as the existence of isomers, multiple charge-states, and magnetic rigidity limits of experimental equipment [40]; however, the former will generally require further experimental work, techniques to deal with multiple charge states [23] have recently been implemented for TOF- $B\rho$ [30], and it is anticipated that FRIB will host the high-rigidity spectrometer with a more than sufficient maximum rigidity, so I do not consider these complications further.

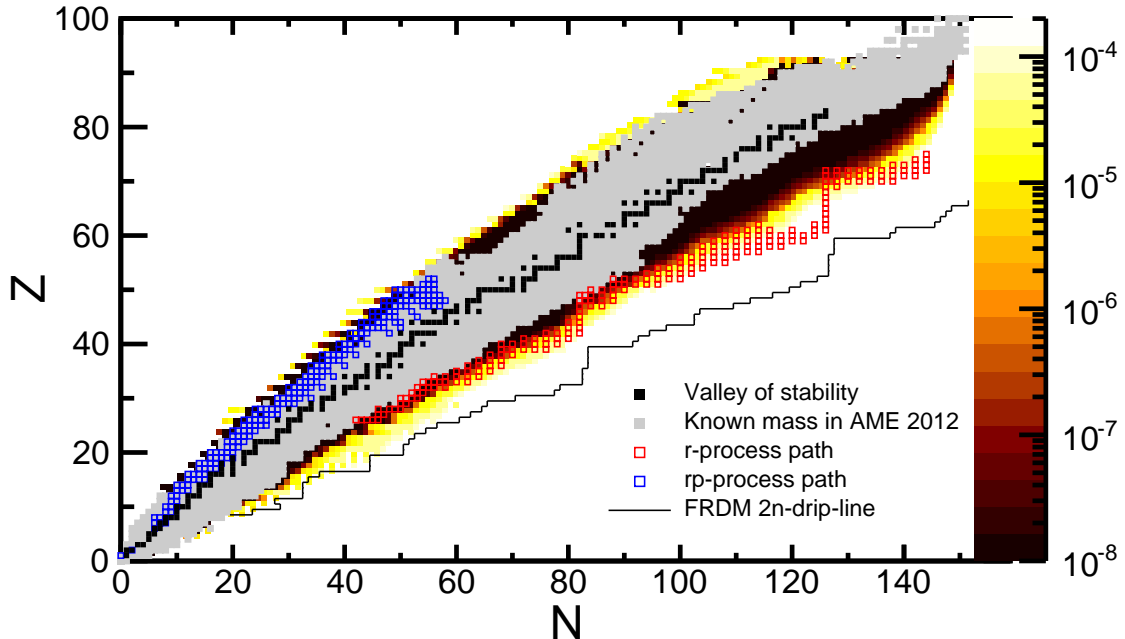


Figure 5. Anticipated relative uncertainty $\delta m/m$ achievable by the combined use of PTMS and the TOF- $B\rho$ method at FRIB. The rp and r -process paths are the same as those referred to in Figure 2. Note that life-time reductions due to particle emission are neglected, and therefore estimates near the proton drip-line are not reliable.

4.4. Estimated precision for FRIB mass measurements

Figure 5 shows the predicted mass measurement precision that can be achieved by the combined use of PTMS and TOF- $B\rho$ at FRIB. Relative to the 1,098 neutron-rich masses reported in the 2012 Atomic Mass Evaluation [45], the predictions shown correspond to 965 higher-precision nuclear masses and 1,172 new nuclear masses on the neutron-rich side of stability: 693 from PTMS with a precision $\leq 10^{-6}$ and 479 from TOF- $B\rho$ with a

precision $\leq 10^{-4}$. These measurements would roughly double the known mass surface for neutron-rich nuclides, leading to advances in nuclear structure and nuclear astrophysics. Masses will likely be obtained very near to the neutron drip-line up to roughly iron and will elucidate the evolution of the $N = 82$ and (especially) $N = 126$ shell-closures for decreasing proton numbers. The expansion of the mass surface up to $A \approx 100$ will tightly constrain the possible strength of nuclear heating and cooling in the crusts of accreting neutron stars [9]. Whereas the expansion for the isotopes above iron may deliver nuclear masses along the majority of the r -process path, possibly distinguishing between hot and cold r -process sites, for example with the neodymium masses [51].

5. Conclusions

The TOF- $B\rho$ method has played and will continue to play a key role in mass spectrometry for exotic nuclides. Over the past three decades, such measurements have made significant contributions to our understanding of nuclear structure and nuclear astrophysics, particularly involving neutron-rich nuclides. Though lower precision than other available methods, TOF- $B\rho$ measurements continue to map the frontiers of the nuclear mass surface.

Acknowledgments

I thank my many TOF- $B\rho$ mass measurement collaborators, especially Sebastian George, Alfredo Estradé, Mike Famiano, Wolfi Mittig, Fernando Montes, Hendrik Schatz, and Dan Shapira. This work was supported in part by the U.S. Department of Energy Office of Science under Grants No. DE-FG02-88ER40387 and DESC0019042 and the U.S. National Science Foundation through Grant No. PHY-1430152 (Joint Institute for Nuclear Astrophysics – Center for the Evolution of the Elements).

References

- [1] Leistenschneider E *et al.* 2018 *Phys. Rev. Lett.* **120** 062503
- [2] Michimasa S *et al.* 2018 *Phys. Rev. Lett.* **121** 022506
- [3] Mougeot M *et al.* 2018 *Phys. Rev. Lett.* **120**(23) 232501 URL <https://link.aps.org/doi/10.1103/PhysRevLett.120.232501>
- [4] Ong W J, Valverde A A, Brodeur M, Bollen G, Eibach M, Gulyuz K, Hamaker A, Izzo C, Puentes D, Redshaw M, Ringle R, Sandler R, Schwarz S, Sumithrarachchi C S, Surbrook J, Villari A C C and Yandow I T 2018 *Phys. Rev. C* **98** 065803
- [5] Valverde A A, Brodeur M, Bollen G, Eibach M, Gulyuz K, Hamaker A, Izzo C, Ong W J, Puentes D, Redshaw M, Ringle R, Sandler R, Schwarz S, Sumithrarachchi C S, Surbrook J, Villari A C C and Yandow I T 2018 *Phys. Rev. Lett.* **120** 032701
- [6] Orford R, Vassh N, Clark J A, McLaughlin G C, Mumpower M R, Savard G, Surman R, Aprahamian A, Buchinger F, Burkey M T, Gorelov D A, Hirsh T Y, Klimes J W, Morgan G E, Nystrom A and Sharma K S 2018 *Phys. Rev. Lett.* **120** 262702
- [7] Vilen M, Kelly J M, Kankainen A, Brodeur M, Aprahamian A, Canete L, Eronen T, Jokinen A,

- Kuta T, Moore I D, Mumpower M R, Nesterenko D A, Penttilä H, Pohjalainen I, Porter W S, Rinta-Antila S, Surman R, Voss A and Nyström J 2018 *Phys. Rev. Lett.* **120** 262701
- [8] Iliadis C 2019 *Phys. Rev. C* **99** 065809
- [9] Meisel Z, Deibel A, Keek L, Shternin P and Elfriz J 2018 *J. Phys. G* **45** 093001
- [10] Rüster S B, Hempel M and Schaffner-Bielich J S 2006 *Phys. Rev. C* **73** 035804
- [11] Lunney D 2019 *Hyperfine Interactions* **240** 48 ISSN 1572-9540
- [12] Meisel Z and George S 2013 *International Journal of Mass Spectrometry* **349-350** 145 – 150 ISSN 1387-3806 100 years of Mass Spectrometry URL <http://www.sciencedirect.com/science/article/pii/S1387380613001139>
- [13] Möller P, Nix J R, Myers W D and Swiatecki W J 1995 *Atomic Data and Nuclear Data Tables* **59** 185
- [14] Schatz H 2006 *Int. J. Mass Spectrom.* **251** 293–299
- [15] Schatz H 2005 *Nucl. Phys. A* **758** 607–614
- [16] Lau R, Beard M, Gupta S S, Schatz H, Afanasjev A V, Brown E F, Deibel A, Gasques L R, Hitt G W, Hix W R, Keek L, Möller P, Shternin P S, Steiner A W, Wiescher M and Xu Y 2018 *Astrophys. J.* **859** 62
- [17] Meisel Z *et al.* 2016 *Phys. Rev. C* **93** 035805
- [18] Stein S 2012 *Analytical Chemistry* **84** 7274–7282
- [19] Press W H, Teukolsky S A, Vetterling W T and Flannery B P 1992 *Numerical Recipes in C: The Art of Scientific Computing* 2nd ed (Cambridge University Press)
- [20] Matoš M, Estradé A, Schatz H, Bazin D, Famiano M, Gade A, George S, Lynch W G, Meisel Z, Portillo M, Rogers A, Shapira D, Stolz A, Wallace M and Yurkon J 2012 *Nucl. Instrum. Meth. Phys. Res. Sec. A* **696** 171–179
- [21] Bianchi L, Fernandez B, Gastebois J, Gillibert A, Mittig W and Barrette J 1989 *Nucl. Instrum. Meth. Phys. Res. Sec. A* **276** 509–520
- [22] Wouters J M, Vieira D J, Wollnik H, Enge H A, Kowalski S and Brown K L 1985 *Nucl. Instrum. Meth. Phys. Res. Sec. A* **240** 77–90
- [23] Tarasov O B, Portillo M, Amthor A M, Baumann T, Bazin D, Gade A, Ginter T N, Hausmann M, Inabe N, Kubo T, Morrissey D J, Nettleton A, Pereira J, Sherrill B M, Stolz A and Thoennessen M 2009 *Phys. Rev. C* **80** 034609
- [24] Sarazin F, Savajols H, Mittig W, Nowacki F, Orr N A, Ren Z, Roussel-Chomaz P, Auger G, Baiborodin D, Belozyorov A V, Borcea C, Caurier E, Dlouhý Z, Gillibert A, Lalleman A S, Lewitowicz M, Lukyanov S M, de Oliveira F, Penionzhkevich Y E, Ridikas D, Sakurai H, Tarasov O and de Vismes A 2000 *Phys. Rev. Lett.* **84** 5062–5065
- [25] Savajols H, Jurado B, Mittig W, Baiborodin D, Catford W, Chartier M, Demonchy C E, Dlouhy Z, Gillibert A, Giot L, Khouaja A, Lépine-Szily S, Lukyanov A, Mrazek J, Orr N, Penionzhkevich Y, Pita S, Rousseau M, Roussel-Chomaz P and Villari A C C 2005 *European Physical Journal A Supplement* **25** 23–26
- [26] Meisel Z *et al.* 2015 *Phys. Rev. Lett.* **114** 022501
- [27] Gaodefroy L, Mittig W, Orr N A, Varet S, Chartier M, Roussel-Chomaz P, Ebran J P, Fernández-Domínguez B, Frémont G, Gangnant P, Gillibert A, Grévy S, Libin J F, Maslov V A, Paschalis S, Pietras B, Penionzhkevich Y E, Spitaels C and Villari A C C 2012 *Phys. Rev. Lett.* **109** 202503
- [28] Estradé A *et al.* 2011 *Phys. Rev. Lett.* **107** 172503
- [29] Meisel Z *et al.* 2015 *Phys. Rev. Lett.* **115** 162501
- [30] Estrade A 2019 *ECT* Trento: Nuclear and astrophysics aspects for the rapid neutron capture process in the era of multimessenger observations* July 1-5
- [31] Bollen G, Hausmann M, Sherrill B M and Tarasov O B 2011 *FRIB Estimated Rates v1.06*
- [32] Koura H, Tachibana T, Uno M and Yamada M 2005 *Prog. Theor. Phys.* **113** 305
- [33] Sümmerer K and Blank B 2000 *Phys. Rev. C* **61** 034607
- [34] Tarasov O B 2005 Lise++ development: Abrasion-fission Tech. Rep. MSUCL-1300 National

Superconducting Cyclotron Laboratory

- [35] Tarasov O B and Bazin D 2008 *Nucl. Instrum. Meth. B* **266** 4657
- [36] Ringle R, Schwarz S and Bollen B 2013 *Int. J. Mass Spectrom.* **349-350** 87
- [37] Blaum K, Dilling J and Nörtershäuser W 2013 *Phys. Scripta* **T152** 014017
- [38] Minaya Ramirez E *et al.* 2012 *Science* **337** 1207
- [39] Smith M *et al.* 2008 *Phys. Rev. Lett.* **101** 202501
- [40] Lunney D, Pearson J M and Thibault C 2003 *Reviews of Modern Physics* **75** 1021–1082
- [41] Bollen G 2001 *Nuc. Phys. A* **693** 3
- [42] Tuli J K 2011 Nuclear wallet cards Tech. rep. National Nuclear Data Center 8th Edition
- [43] Möller P, Pfeiffer B and Kratz K L 2003 *Phys. Rev. C* **67** 055802
- [44] Redshaw M, Bollen G, Bustabad S, Kwiatkowski A A, Lincoln D L, Novario S J, Ringle R, Schwarz S and Valverde A A 2013 *Nucl. Instrum. Meth. B* **317** 510
- [45] Audi G, Wang M, Wapstra A, Kondev F, MacCormick M, Xu X and Pfeiffer B 2012 *Chin. Phys. C* **36** 1287
- [46] Mumpower M *et al.* 2016 *Prog. Part. Nucl. Phys.* **86** 86
- [47] Kankainen A, Äystö J and Jokinen A 2012 *J. Phys. G Nucl. Partic.* **39** 09310
- [48] Kwiatkowski A A, Bollen G, Redshaw M, Ringle R and Schwarz S 2015 *Int. J. Mass Spectrom.* **379** 9
- [49] Eliseev S *et al.* 2015 *Phys. Rev. Lett.* **115** 062501
- [50] Savajols H 2001 *Hyperfine Interactions* **132** 243–252
- [51] Mumpower M R, McLaughlin G C, Surman R and Steiner A W 2016 The Link between Rare-Earth Peak Formation and the Astrophysical Site of the R Process